Genetic Analysis Demonstrates a Direct Link Between Rho Signaling and Nonmuscle Myosin Function During Drosophila Morphogenesis

Susan R. Halsell, Benjamin I. Chu and Daniel P. Kiehart

Department of Cell Biology, Duke University Medical Center, Durham, North Carolina 27710

Manuscript received October 22, 1999
Accepted for publication March 29, 2000

ABSTRACT

A dynamic actomyosin cytoskeleton drives many morphogenetic events. Conventional nonmuscle myosin-II (myosin) is a key chemomechanical motor that drives contraction of the actin cytoskeleton. We have explored the regulation of myosin activity by performing genetic screens to identify gene products that collaborate with myosin during Drosophila morphogenesis. Specifically, we screened for second-site noncomplementors of a mutation in the *zipper* gene that encodes the nonmuscle myosin-II heavy chain. We determined that a single missense mutation in the *zipper*^{Ebr} allele gives rise to its sensitivity to second-site noncomplementation. We then identify the Rho signal transduction pathway as necessary for proper myosin function. First we show that a lethal *P*-element insertion interacts genetically with *zipper*. Subsequently we show that this second-site noncomplementing mutation disrupts the *RhoGEF2* locus. Next, we show that two EMS-induced mutations, previously shown to interact genetically with *zipper*^{Ebr}, disrupt the *RhoA* locus. Further, we have identified their molecular lesions and determined that disruption of the carboxyl-terminal CaaX box gives rise to their mutant phenotype. Finally, we show that *RhoA* mutations themselves can be utilized in genetic screens. Biochemical and cell culture analyses suggest that Rho signal transduction regulates the activity of myosin. Our studies provide direct genetic proof of the biological relevance of regulation of myosin by Rho signal transduction in an intact metazoan.

MORPHOGENESIS encompasses a complex array of cell shape changes, rearrangements, and movements at many stages throughout the life cycle of an organism. The dynamic cytoskeleton drives many of these cellular events, and regulation of the cytoskeleton during morphogenesis is likely a multistep process. Morphogenetic cytoskeletal changes or movements may occur in a cell-autonomous fashion in response to differentiation cues. Alternatively, these cytoskeletal changes may be induced downstream of extracellular cues. Indeed, it is likely that any given morphogenetic process requires a combination of both cell-autonomous and nonautonomous processes. In either case, intracellular signal transduction leading to direct reconfiguration of cytoskeletal structure and activity would be required. As such, understanding morphogenesis requires investigation of the interplay between upstream regulation and cytoskeletal dynamics in an intact animal.

The actin cytoskeleton plays a special role in epithelial sheet morphogenesis. During vertebrate neurulation, neural tube formation is a multistep process, and cell shape changes occur at the dorsal and medial hingepoints (reviewed in Schoenwolf and Smith 1990). Electron microscopy reveals actin filaments in these neuroepithelial cells undergoing wedging; additional studies reveal that cytochalasin D treatment can disrupt dorsal-lateral hingepoint cell wedging, followed by disruption of neural fold convergence. Pharmacological and genetic studies in Drosophila reveal that the actin cytoskeleton is critical for many developmental processes, including mRNA localization, nuclear migrations, and cellularization in the early embryo (reviewed in Miller 1995). The role of the actin cytoskeleton during morphogenesis has also been examined in *Caenorhabditis elegans*. During the early morphogenetic events of ventral enclosure and elongation, specific subcellular actin arrays are observed (Preiss and Hirsh 1986; Williams-Masson *et al.* 1997). Cytochalasin D treatment disrupts these arrays and both morphogenetic movements fail. These studies suggest that contraction of the actin cytoskeleton drives the completion of ventral enclosure and elongation. Nevertheless, the molecular motor that drives cell shape changes and rearrangements in *C. elegans* has not been identified.

Conventional, nonmuscle myosin-II (henceforth, myosin), a chemomechanical motor, drives contraction of the actin cytoskeleton. Myosin functions throughout phylogeny, driving cell shape changes required for cytokinetic furrow formation, cell movement, and tissue morphogenesis. The role of myosin in these processes may be inferred from its subcellular location. In addition, mutagenesis of myosin genes in several organisms (including Drosophila, see below) reveals its critical function in these processes. The MYO1 gene encodes the *Saccharomyces cerevisiae* myosin-II heavy chain, and

Corresponding author: Daniel P. Kiehart, Duke University Medical Center, Department of Cell Biology, Research Dr., 307 Nanaline Duke Bldg., Durham, NC 27710. E-mail: d.kiehart@cellbio.duke.edu

MYO1 mutants exhibit retarded cell growth (Watts *et al.* 1987). Mutants also fail to form actomyosin contractile rings, but cytokinesis by alternative means still occurs (Bi *et al.* 1998). Myosin function in *Dictyostelium discoideum* has been disrupted by mutating the heavy chain gene via homologous recombination and by antisense RNA inactivation (De Lozanne and Spudich 1987; Knecht and Loomis 1987; Manstein *et al.* 1989). These studies reveal that fruiting body morphogenesis is disrupted and that lack of myosin function blocks formation of the stalk at the mound stage. Microscopic analysis suggests that cell shape changes driven by myosin function are critical during Dictyostelium morphogenesis (Knecht and Shelden 1995; Shelden and Knecht 1996). Similar to the yeast study, adhesive Dictyostelium myosin-II null cells can undergo cytokinesis in the absence of myosin-II function; however, cells in suspension absolutely require myosin-II function for cytokinesis (Neujahr *et al.* 1997; Zang *et al.* 1997).

Genetic and experimental studies in *Drosophila melanogaster* reveal multiple steps in the life cycle that require myosin function. Myosin is subcellularly localized in embryonic cells undergoing apical constriction (Young *et al.* 1991, 1993; Edwards and Kiehart 1996; Kiehart *et al.* 2000). Zygotic activity of the single copy, nonmuscle myosin-II heavy chain gene (*zipper*) is absolutely required for enclosure of the amnioserosa by the lateral epidermis during dorsal closure (Young *et al.* 1993). It was noted that ventral enclosure in *C. elegans* resembles dorsal closure and may also require a myosin motor (Williams-Masson *et al.* 1997). Embryonically, *zipper* also functions during head involution and axon guidance (Côté *et al.* 1987; Zhao *et al.* 1988; Jack and Myette 1997; Pederson 1997; Blake *et al.* 1998). Further genetic manipulation reveals that border cell migration and nurse cell transport during oogenesis, nuclear migrations in the early embryo, larval cytokinesis, and pupal imaginal disc morphogenesis also require myosin function (Gotwals and Fristrom 1991; Karess *et al.* 1991; Wheatley *et al.* 1995; Edwards and Kiehart 1996; Halsell and Kiehart 1998). In fact, depletion of myosin during leg imaginal disc morphogenesis results in deformed adult legs, referred to as the malformed phenotype (mlf, described below; Edwards and Kiehart 1996).

Pupal leg imaginal disc morphogenesis results from myosin-driven cell shape changes, and it is particularly sensitive to perturbation (reviewed in von Kalm *et al.* 1995; Gotwals and Fristrom 1991; Edwards and Kiehart 1996; Halsell and Kiehart 1998). No significant cell proliferation or rearrangements (relative to the cells' contacts with their nearest neighbors) are observed in the prepupal leg imaginal disc; instead the early phase of leg disc elongation appears to rely on the change in cell shapes from anisometric to isometric (Condic *et al.* 1990). Disruption of these cell shape changes gives rise to the mlf phenotype that is readily identifiable in the adult (Figure 3). We exploited the sensitivity of leg imaginal disc morphogenesis by testing whether Deficiencies for genomic regions uncover loci that genetically interact with *zipper* (Halsell and Kiehart 1998). In that study, we found 2 deficiencies that genetically interact strongly and 17 that interact at intermediate levels. Within this collection of deficiencies, we have thus far identified 3 whose interaction with *zipper* can be explained by individual mutant loci. These three loci include *cytoplasmic tropomyosin*, *viking* (encoding a collagen IV), and a single complementation group represented by two EMS-induced alleles (*E3.10* and *J3.8*).

Here, we determined that the $zipper^{Ebr}$ (zip^{Ebr}) allele used in our screens has a single missense mutation within the region encoding the globular head domain. Further, we identified two zip^{Ebr} genetic interactors that encode members of the Rho signal transduction pathway. First, we screened lethal *P*-element transposon insertions and found that a *P*-element insertion that disrupts the *RhoGEF2* (*Rho Guanine Exchange Factor 2*) locus interacts genetically with *zipper*. We also show that the complementation group defined by the *E3.10* and *J3.8* mutations encodes RhoA. DNA sequence analysis of these two EMS-induced mutations reveals single point mutations within the *RhoA* gene. Finally, we detected genetic interactions between the *RhoA* mutation and a flanking chromosomal deficiency. Overall, these results verify a direct, *in vivo* link between the Rho signal transduction pathway and myosin function.

MATERIALS AND METHODS

Stocks: We obtained a collection of second chromosome lethal *P*-element insertions, $w^a\ N^{fa\text{-}g}$; *Df(2R)Jp1/CyO*, $w^a\ N^{fa\text{-}g}$; *Df(2R)Jp4/CyO* and $w^a\ N^{fa\text{-}g}$; Df*(2R)Jp8/CyO* stocks from the Bloomington Stock Center (Bloomington, IN). Bill Saxton (Indiana University) provided $w^a\ N^{fa\text{-}g}$; *E3.10/CyO* (Saxton *et al.* 1991). Ruth Steward (Rutgers University) provided *J3.8/CyO* (R. Steward, personal communication). We obtained the *w*; $RhoGEF2^{1.1}$/*CyO* and *w*; $RhoGEF2^{4.1}$/*CyO* stocks from J. Settleman (Massachusetts General Hospital Cancer Center, Harvard Medical School; Barrett *et al.* 1997). M. Mlodzik (European Molecular Biology Laboratory) provided *y w*; $RhoA^{72F}$/*CyO* and *y w*; $RhoA^{72O}$/*CyO* (Strutt *et al.* 1997). zip^{Ebr}/*SM5* was obtained from Jim Fristrom (University of California, Berkeley; Gotwals and Fristrom 1991; Gotwals 1992).

Genetic screens and complementation analysis: All crosses were performed at 25° on standard cornmeal/molasses fly food. The second-site noncomplementation screen was performed as previously described (Halsell and Kiehart 1998). Five zip^{Ebr}/*SM5* virgin females were mated to three to five mutation- or deficiency-bearing males. Crosses were brooded every 4–5 days. All progeny were scored for the malformed phenotype (Gotwals and Fristrom 1991). Penetrance of the malformed phenotype in flies double heterozygous for the mutation or deficiency and zip^{Ebr} (*e.g.*, *m* + / + zip^{Ebr}) was compared directly to sibling flies singly heterozygous for either of the mutations (*e.g.*, *m* + / *SM5* or + zip^{Ebr}/*Balancer*). In no cases did flies singly heterozygous for the mutation or deficiency result in a significant number of malformed flies.

Genetic complementation was performed by crossing five

balanced virgin females to three to five balanced males. All progeny were scored. Since *Balancer*/*Balancer* progeny are embryonic and/or early larval lethal, the Mendelian expectation for mutations that complement one another is that 33% of the adult progeny will carry both mutations.

***P*-element reversion:** Specificity of the *l(2)04291* interaction with zip^{Ebr} was verified by excision of the *P* element and reversion of (1) the malformed phenotype in double heterozygous flies and (2) the homozygous lethality of the original *l(2)04291* chromosome. Briefly, *cn l(2)04291*/*CyO*; ry^{506} males were mass-mated to *Sp*/*CyO*; *Sb* Δ *2-3*/*TM6* virgins. In the F_1 generation, individual *cn l(2)04291*/*CyO*; *Sb* Δ *2-3*/ry^{506} males were mated to *Bc Elp*/*CyO*; *ry* virgins. In the F_2 generation, excision events were identified as a loss of the ry^+ marker within the *P* element. From each line exhibiting *ry* males, individual *cn* $l(2)04291^{rev}$/*Bc Elp* or *CyO*; *ry* males were mated to *cn* zip^{Ebr}/*SM5* virgins. In the next and subsequent generations, reversion of the genetic interaction with zip^{Ebr} was observed as a loss of the malformed phenotype in *cn* $l(2)04291^{rev}$ + /*cn* + zip^{Ebr} double heterozygous flies. Stocks were established for each of the $l(2)04291^{rev}$ lines, and each was tested for homozygous viability and in complementation assays with the original *l(2)04291* chromosome.

Plasmid rescue: Genomic DNA flanking the *P*-element insertion site was recovered by plasmid rescue, using established methods. In brief, genomic DNA was isolated from *cn l(2)04291*/*CyO* flies and quantified by its absorbance at 260 nm (Lis *et al.* 1983). A total of 1 μg was digested with *Xba*I and *Spe*I for 4 hr, and the enzymes were heat inactivated by incubation at 65° for 20 min, followed by ethanol precipitation. The DNA pellet was resuspended in 15 μl TE, and 5 μl was ligated overnight at 15° in a 200-μl reaction containing 3 units of T4 DNA ligase (GIBCO BRL, Gaithersburg, MD). The ligated product was ethanol precipitated, resuspended in 10 μl H_2O, and the entire resuspension was used to transform XL-1 Blue-competent bacteria (Stratagene, La Jolla, CA). Transformants were selected on LB-kanamycin plates. The insert DNA was subcloned in Bluescript (Stratagene) as *Hin*dIII fragments, and these subclones were sequenced with Bluescript-specific primers at the Duke University Comprehensive Cancer Center DNA analysis facility (see below).

DNA sequencing of the zip^{Ebr}, *E3.10*, and *J3.8* mutations: Homozygous mutant animals were collected as follows. Overnight egglays were performed, and the embryos were allowed to age for at least 24 hr at 25°. zip^{Ebr} homozygotes were collected from a *y*; zip^{Ebr}/*CyO*, y^+ stock and were identified as *y* embryos and/or larvae. Mutant *E3.10* and *J3.8* embryos were collected on the basis of the characteristic head involution defect assayed at 20× with a stereomicroscope (Figure 5). Genomic DNA was then isolated as follows. Twenty animals were homogenized in 50 μl of 10 mm Tris-Cl, pH 8.2, 1 mm EDTA, 25 mm NaCl, 200 μg/ml proteinase K by pressing the embryos against the tube wall with a P-200 ("yellow") tip. The homogenate was digested at 37° for 20 min, and then the proteinase K was heat inactivated by incubation for 2 min at 98° (Gloor *et al.* 1993). The debris was pelleted in the microfuge and the DNA-containing supernatant was used in the PCR reactions.

Fragments of DNA spanning either the *zipper* or *RhoA* genes were generated by PCR. *zipper*-specific primers were based on the complete genomic sequence (Mansfield *et al.* 1996). *RhoA*-specific primers were based on the previously published cDNA sequence for *RhoA* and *RhoL* and intron sequences determined in this study (Hariharan *et al.* 1995; Murphy and Montell 1996). Each 30-μl PCR reaction included 3 μl of the 50-μl mutant genomic DNA preparation, 40 mm KCl, 60 mm Tris-Cl, pH 8.5, 166 μm dNTPs, 25 ng of each primer, 1.5–6.0 mm $MgCl_2$, 0.2 μl of Perfect Match (Stratagene), and 0.3 μl of BIO-X-ACT DNA polymerase (ISC BioExpress, Kaysville, UT). The PCR reactions were performed in a MJ Research thermocycler as follows: 5 min at 95°, followed by 35 cycles of 1 min at 95°, 1 min at 58°, 5 min at 72°, and finally a cycle of 10 min at 72°. Typically, at least three PCR reactions were combined, run on an agarose gel, and eluted from gel slices with QIAGEN spin columns (QIAGEN, Valencia, CA). DNA sequencing was performed by the Duke University Comprehensive Cancer Center DNA analysis facility using an ABI Prism 377XL DNA sequencer and dRhodamine/BigDye terminator cycle sequencing reagents (PE Applied Biosystems, Foster City, CA).

Protein sample preparation and immunoblotting: Twenty appropriately staged embryos or larvae were collected from egg-lay plates, homogenized in 100 μl 1× sample buffer, and boiled for 3 min. SDS-PAGE and immunoblotting were performed essentially as in Kiehart and Feghali (1986), with the following modifications. Aliquots (15 μl) of total embryo homogenate in sample buffer (~3 embryo equivalents) were separated in 3-mm lanes on 6%/0.6% acrylamide gels by SDS-PAGE. Blots were blocked with Blotto (5% nonfat milk, 0.02% sodium azide, 0.2% Tween-20), and all antibody incubations were in Blotto. Primary antibody dilutions were 1:500 and included rabbit polyclonal antisera directed against myosin heavy chain (656; Kiehart and Feghali 1986) or α-spectrin (905; Byers *et al.* 1987). Signal detection was performed by incubation with horseradish peroxidase conjugated secondary antibodies (1:500; Chemicon International, Temecula, CA), followed by incubation with SuperSignal substrate (Pierce, Rockford, IL) according to manufacturer's directions. Exposures were typically 1–2 min.

Mounting of adult legs and wings and embryonic cuticles: Malformed adults were preserved in 70% ethanol. Legs and/or wings were removed and mounted in CMPC10 (PolySciences, Warrington, PA). The legs and wings were observed by brightfield microscopy, using a 5× Neofluar objective [0.15 numerical aperture (NA)] on a Zeiss Axioplan microscope. Background subtracted images were captured with a Hamamatsu 4880 cooled CCD camera and Metamorph software (Kiehart *et al.* 1994). Contrast was adjusted using Adobe Photoshop software and images were montaged and labeled.

Embryonic cuticles were mounted as follows. Overnight egglays were performed on standard grape juice plates. The embryos were subsequently aged for 36–48 hr at 25°. Unhatched, brown embryos were hand dechorionated on double-stick tape and mounted in a drop of 8.4% polyvinyl alcohol (Sigma, St. Louis), 22% lactic acid, and 22% phenol (PVLP; Pederson *et al.* 1996). Alternatively, recently hatched Canton-S larvae were mounted in a drop of Hoyers mountant, diluted 1:1 with lactic acid (Wieschaus and Nüsslein-Volhard 1986). The mounts were weighted and allowed to harden overnight at 65°. The cuticles were imaged by phase-contrast microscopy, using a 10× Plan-Neofluar objective (0.3 NA) or 20× Achroplan objective (0.45 NA). Image capturing was as above.

RESULTS

zip^{Ebr} is the *zipper* allele most sensitive to second-site noncomplementation in genetic interaction screens: Previous studies revealed that putative null alleles of *zipper* do not exhibit second-site noncomplementation behavior; in contrast, zip^{Ebr} and two postembryonic lethal zipper alleles ($zip^{2.1}$ and $zip^{6.1}$) do (Halsell and Kiehart 1998; J. Fristrom and S. R. Halsell, unpublished results). zip^{Ebr} is more sensitive than either $zip^{2.1}$ or $zip^{6.1}$. The zip^{Ebr} allele was generated by EMS mutagenesis and was identified in screens for mutations that interact

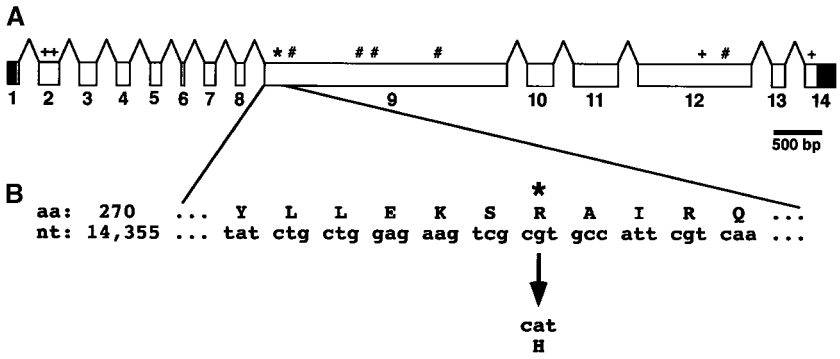

Figure 1.—Genomic organization of the *zipper* locus and the molecular lesion in zip^{Ebr}. (A) The *zipper* locus is a 21-kb transcription unit comprised of 14 exons and encodes a transcript ~6 kb long (Ketchum *et al.* 1990; Mansfield *et al.* 1996). Sequence analysis of the zip^{Ebr} open reading frame and splice junctions revealed a single missense mutation (*) in exon 9 and a total of five silent mutations (#) relative to the sequence determined by the Berkeley Drosophila Genome Project (BDGP; accession no. AC006244; Berkeley Drosophila Genome Project, unpublished results). In addition, we found four irregularities (+) between the *zipper* sequence determined in this study and by the BDGP as compared to the previous reported sequences for the *zipper* cDNA and genomic sequence (Ketchum *et al.* 1990; Mansfield *et al.* 1996). Specifically, we and the BDGP find that exon 2 lacks a CC pair at position 989/990 and a T nucleotide at position 1028 [numbering relative to the genomic sequence in Mansfield *et al.* (1996)]. These changes give rise to a loss of 1 codon and a frameshift over 12 codons until the sequence reenters frame after the T deletion. In addition, within exon 12, we found a GC pair at position 18,820/18,821 that is inverted relative to the other published sequences. This change encodes an aspartic acid-arginine instead of glutamic acid-glycine. Finally, we find a single nucleotide change in exon 14 at position 20,248 that encodes a glycine instead of serine residue.

genetically with the *Broad-Complex* (Gotwals and Fristrom 1991).

To determine the molecular lesion associated with the genetic behavior of zip^{Ebr}, we sequenced genomic DNA isolated from zip^{Ebr} homozygotes. All intron/exon boundaries in the mutant zip^{Ebr} locus are wild type. We identified five silent mutations, relative to the sequence determined by the Berkeley Drosophila Genome Project (accession no. AC006244, Berkeley Drosophila Genome Project). Significantly, within the entire open reading frame we found only a single missense mutation located within exon 9 (Figure 1). zip^{Ebr} exhibits a transition mutation at nucleotide 14,374 (relative to the corrected sequence reported in Mansfield *et al.* 1996, accession no. U35816), such that G is changed to A. Such transitions are consistent with those generated by EMS (Ashburner 1989), and in this case, result in an arginine-to-histidine replacement at amino acid 276 (with respect to the corrected, short transcript published in Ketchum *et al.* 1990). This is equivalent to the arginine found at position 274 in the chicken fast skeletal muscle myosin heavy chain (Cope and Hodge 2000). The arginine at this position is highly conserved in all members of the myosin superfamily. Among 130 different myosins, 128/130 of them conserve the arginine residue at this position (Cope and Hodge 2000). On the basis of comparison to the chicken skeletal myosin heavy chain structure determined crystallographically, this residue lies near the wall of the ATP-binding pocket (Rayment *et al.* 1993).

We performed immunoblot analysis to determine if the level of myosin heavy chain protein is altered in zip^{Ebr} mutants. zip^{Ebr} mutants die as late embryos or early larvae, and both stages were examined (Figure 2). The level of myosin heavy chain protein in zip^{Ebr} homozygous mutant embryos is somewhat reduced in comparison to the level seen in wild-type embryos (Figure 2, A and C). Further, the level of myosin heavy chain observed in the zip^{Ebr} homozygous larvae is comparable to that observed in their heterozygous zip^{Ebr} siblings (Figure 2, D and E). This is in marked contrast to that of the apparent null allele, zip^{2}, which is predicted to produce a truncated protein due to a premature stop codon at residue 750 and exhibits little or no detectable myosin heavy chain protein in homozygous mutant embryos (Figure

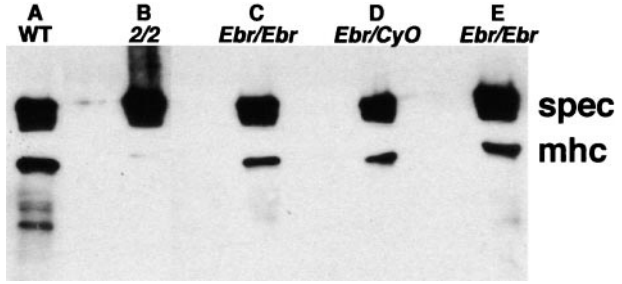

Figure 2.—Immunoblot analysis reveals myosin heavy chain protein levels in zip^{Ebr} homozygous mutant animals. Animals homozygous mutant for zip^{Ebr} die as late embryos/early larvae; therefore, myosin heavy chain levels were examined in both stages. Protein levels were compared between comparably staged wild-type, zip^{Ebr}, and zip^{2} homozygous mutant animals. The wild-type embryo controls (lane A, WT) were derived from Canton-S stocks, while the phenotypically wild-type larvae (lane D, Ebr/CyO) were the zip^{Ebr}/CyO, y^{+}-bearing siblings of the mutant larvae. In addition to staining with polyclonal anti-myosin heavy chain antibody (mhc), we also stained with a polyclonal antibody directed against α-spectrin (spec) as a loading control that suggests minor variation in total protein loaded. Levels of myosin heavy chain protein in zip^{Ebr} homozygous mutant animals (lane C, Ebr/Ebr embryos and lane E, Ebr/Ebr larvae) are somewhat reduced as compared to the levels in wild type. This level of 205-kD heavy chain is significantly greater than that observed in zip^{2} homozygotes (lane B, 2/2 embryos). The molecular lesion in zip^{2} is a premature stop codon that should give rise to a ~85-kD protein (Mansfield *et al.* 1996); any detectable full-length myosin heavy chain may result from read-through or more likely reflects perdurance of the maternally encoded protein.

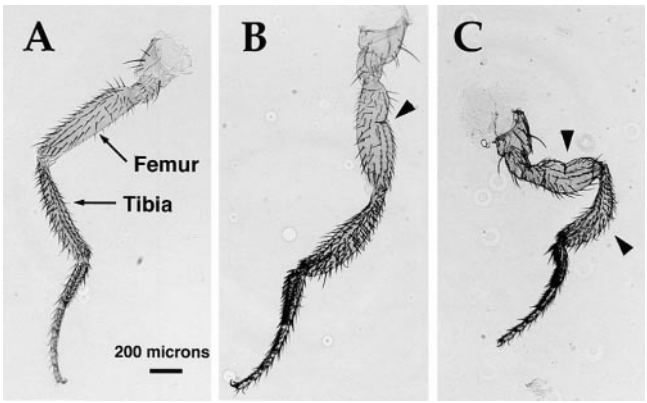

Figure 3.—Genetic interactions between *RhoGEF2* and *zipper* and between *RhoA* and *zipper* cause defects in leg imaginal disc morphogenesis that give rise to the malformed leg phenotype. (A) The third leg of a wild-type adult consists of tarsal segments, the tibia, and the femur. The tibia and femur (arrows) are long, slender structures, and morphogenetic cell shape changes drive their elongation (Condic *et al.* 1990). (B and C) The malformed leg phenotype exhibits variable expressivity. (B) In less severe cases, a dent in the femur or tibia (arrowhead) is diagnostic. This fly was genotypically $RhoGEF2^{4.1}$ +/+ zip^{Ebr}. (C) In more severe cases, a dent and twisting of the femur is apparent, along with shortening and thickening of the tibia (arrowheads). This fly was double heterozygous for $RhoA^{E3.10}$ and zip^{Ebr}. Note that flies from any given cross giving rise to progeny double heterozygous for either *RhoGEF2* or *RhoA* and zip^{Ebr} show the entire range of malformed phenotypes. Similar results are obtained with all of the tested *RhoGEF2* and *RhoA* alleles. These images were captured using brightfield microscopy and a 5× Neofluar objective (0.15 NA). The scale is the same in A–C.

2B; Young *et al.* 1993; Mansfield *et al.* 1996). Any residual, full-length myosin heavy chain protein in zip^2 homozygotes is due to read-through or more likely reflects perdurance of wild-type protein loaded maternally. zip^2/+ heterozygous flies do not display second-site noncomplementation in our assay. We conclude that the dominant behavior of the zip^{Ebr} allele in the mlf second-site noncomplementation is probably due to the unique structure of the R276H substituted zip^{Ebr} gene product and not likely to arise from a reduction in myosin heavy chain protein levels.

***RhoGEF2* interacts genetically with *zipper*:** To identify loci encoding gene products that collaborate with nonmuscle myosin during morphogenesis, we performed second-site noncomplementation screens for the mlf leg phenotype (Figure 3; Halsell and Kiehart 1998). We extended our previous chromosomal deficiency screens by screening a collection of 268 single, lethal *P*-element insertional mutations on the second chromosome for genetic interactions with the zip^{Ebr} allele. Fourteen insertions failed to complement zip^{Ebr}. Previously, we arbitrarily defined the strength of the genetic interaction on the basis of the percentage of flies of the appropriate genotype that exhibit the malformed phenotype: weak interactions show penetrance of 10–25% while intermediate interactions are 25–75% penetrant (Halsell and Kiehart 1998). Eleven of the lethal *P*-element insertions we identified are weak interactors. Three of the insertions are intermediate interactors. Two of these intermediate interactors are not second-site noncomplementing loci but are new *zipper* alleles, exhibiting intraallelic complementation (S. R. Halsell, unpublished observations). The third intermediate interacting mutation, *l(2)04291*, causes mlf flies *in trans* to zip^{Ebr} with a penetrance of 38% (Table 1).

Genetic reversion analysis confirmed that the interaction observed between zip^{Ebr} and *l(2)04291* is a direct consequence of the *P*-element insertion. After mobilizing the *P* element by crossing in a transposase source, we established 57 lines that had lost the $rosy^+$ marker. Each line was tested for genetic interaction with zip^{Ebr}. Of these lines, 29 no longer interacted genetically with zip^{Ebr}. All 29 reverted lines are homozygous viable and all complement the original *l(2)04291 P*-element insertion, suggesting that each represents a precise excision of the *P* element. This result demonstrates that the observed genetic interaction with zip^{Ebr} is specific to the transposon insertion. The remaining 28 lines appear to be imprecise excision events. All interact genetically with zip^{Ebr}, are homozygous inviable, and fail to complement the original *P* allele.

We subsequently determined that the *P*-element insertion disrupts the *RhoGEF2* locus. We recovered genomic DNA flanking the *P*-element insertion by plasmid rescue, sequenced flanking DNA, and discovered that the *P* element lies within an intron that interrupts the 5′ UTR of the *RhoGEF2* gene. We made this observation concomitant with the first publications of this *RhoGEF2* locus (Barrett *et al.* 1997; Häcker and Perrimon 1998). To further confirm that the genetic interaction observed with zip^{Ebr} results from a mutation in *RhoGEF2*, two EMS-induced mutant *RhoGEF2* alleles, *1.1* and *4.1* (Barrett *et al.* 1997), were tested in the malformed leg assay. Both alleles interacted with zip^{Ebr}; the penetrance of the malformed phenotype in double heterozygous flies was 33% with the $RhoGEF2^{1.1}$ allele and 27% with the $RhoGEF2^{4.1}$ allele (Table 1), comparable to that seen with the original *P*-insertional allele.

In addition to the malformed legs observed in flies double heterozygous for mutant *RhoGEF2* and zip^{Ebr}, we observed malformed wings at comparable frequencies (Figure 4). Between 80 and 97% of the flies exhibiting a malformed leg phenotype also exhibited malformed wings. In contrast, most other loci that interact with *zipper* do not exhibit significant wing defects (S. R. Halsell, unpublished observation). We rarely observed malformed wings when the legs were wild type. Taken together, these data indicate a requirement for *RhoGEF2* during myosin-driven leg and wing imaginal disc morphogenesis.

Myosin-driven imaginal disc morphogenesis requires RhoA Function: In a previous screen for *zipper* inter-

TABLE 1

RhoA* and *RhoGEF2* mutations behave as second-site noncomplementors of *zip^{Ebr}

Mutation	% malformed (n)[a]		
	+ *zip^{Ebr}*/*m* +	*m* +/+ *SM5*	
RhoGEF2^{04291}[b]	38 (249)	1 (278)	
RhoGEF2$^{1.1}$	33 (380)	<1 (443)	
RhoGEF2$^{4.1}$	27 (427)	0 (535)	
RhoA^{72F}	96 (192)	0 (259)	
RhoA^{72O}	92 (283)	<1 (333)	
RhoA$^{E3.10}$	100 (26)	4 (160)	Halsell and Kiehart (1998)
RhoA$^{J3.8}$	100 (61)	0 (116)	Halsell and Kiehart (1998)
Df(2R)Jp4	90 (93)	4 (230)	
Df(2R)Jp8	98 (86)	2 (156)	Halsell and Kiehart (1998)

[a] Percentage of malformed flies double heterozygous for the indicated mutation and *zip^{Ebr}* (*m* +/+ *zip^{Ebr}*). *n* is the total number of flies of this genotype that were scored. The low number of scored *RhoA$^{E3.10}$* and *RhoA$^{J3.8}$* flies *in trans* to *zip^{Ebr}* reflects the semilethal phenotype of this class.

[b] Lethal *P*-element insertion.

actors, we identified a single complementation group, represented by two independently derived EMS mutations (*E3.10* and *J3.8*), as the locus within *Df(2R)Jp8* responsible for this deficiency's strong second-site noncomplementation and partial synthetic lethality *in trans* to *zip^{Ebr}* (Table 1; Halsell and Kiehart 1998). These mutations were recovered in screens for lethals uncovered by *Df(2R)Jp8*, which deletes the chromosome between cytogenetic positions 52F5-9; 52F10-53A1 (Saxton *et al.* 1991; Z. Liu and R. Steward, personal communication).

We have characterized *E3.10* and *J3.8* further. These alleles are recessive, embryonic lethals; homozygous or trans-heterozygous *E3.10*/*J3.8* mutant embryos have dorsal anterior holes in their cuticle (Figure 5B). Further, mutant allele *E3.10* behaves genetically like a null. When *E3.10* is *in trans Df(2R)Jp8*, mutant embryos show similar cuticular defects as *E3.10* homozygotes (*cf.* Figure 5, B and C).

Interestingly, polytene chromosome *in situ* analysis placed the *RhoA* locus at cytogenetic position 52E3-6 (Strutt *et al.* 1997), adjacent to but not included in the interval removed by *Df(2R)Jp8*. Nevertheless, we suspected that the *E3.10* and *J3.8* mutations might be allelic

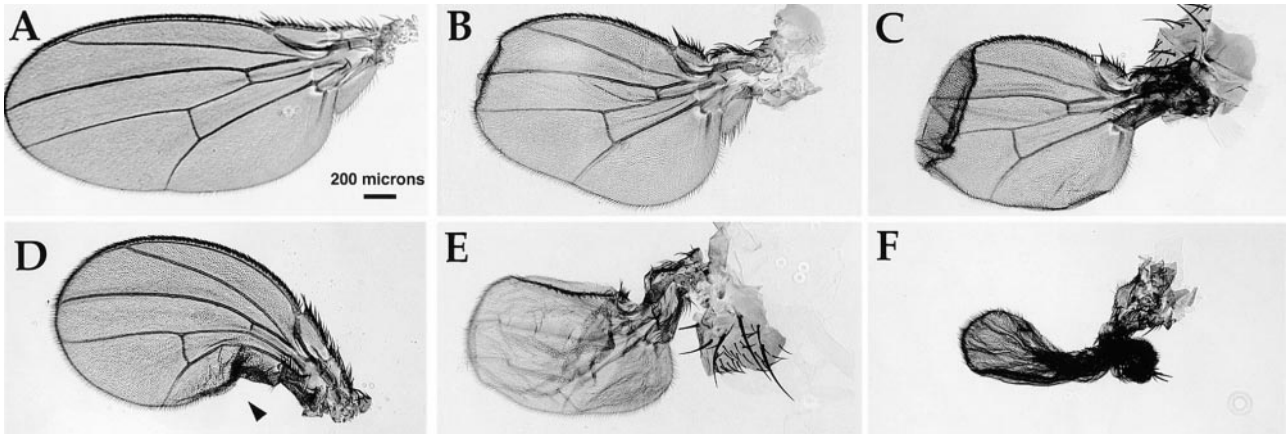

Figure 4.—Genetic interactions between *zipper* and *RhoA* and between *zipper* and *RhoGEF2* give rise to malformed wings. The origin of the morphogenetic defects may include inappropriate cell shape changes, proliferation, and adhesion. As in the case of the leg, a range of malformed wings is generated in any given cross, and the same range is seen whether the fly is carrying *zip^{Ebr} in trans* to *RhoA* or *RhoGEF2*. (A) The wild-type wing is elongated, exhibits tight adhesion between the two cell layers of the wing blade, and a characteristic pattern of wing veins. (B and C) Weak malformed wing phenotypes include a broadening of the wing blade and folding back of the distal portion of the wing blade. (D) Notching of the posterior region of the wing blade also occurs (arrowhead). This phenotype was also observed in genetic interactions between *zip^{Ebr}* and *br^{1}* (Gotwals and Fristrom 1991; Gotwals 1992). (E) In more severe cases, wings lacking adhesion between the wing blade bilayer and any apparent wing venation are observed. (F) In the most severe cases, wings are greatly reduced in size. Genotypes are as follows: (A) Canton-S; (B and E) *RhoA^{72F}* +/+ *zip^{Ebr}*; (C and F) *RhoGEF2$^{4.1}$* +/+ *zip^{Ebr}*; and (D) *RhoA$^{E3.10}$* +/+ *zip^{Ebr}*. These images were captured using brightfield microscopy and a 5× Neofluar objective (0.15 NA). The scale is the same in all panels.

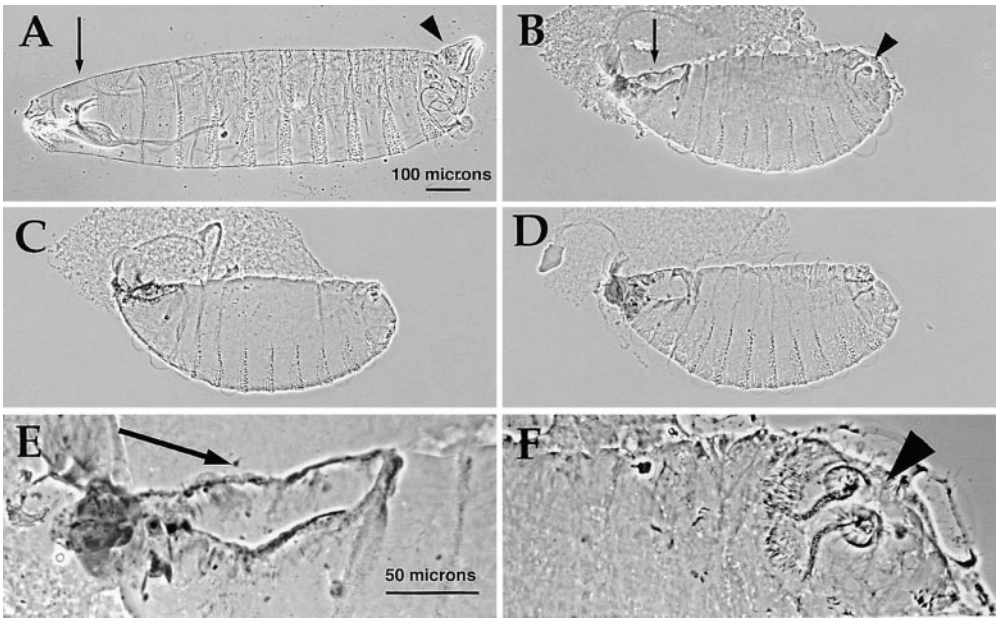

Figure 5.—*RhoA* mutant embryos exhibit dorsal anterior holes. Cuticle preparations were made of (A) a newly hatched wild-type first instar larva; and (B, E, and F) $RhoA^{E3.10}/RhoA^{E3.10}$ homozygous, (C) $RhoA^{E3.10}/Df(2R)Jp8$ trans-heterozygous, and (D) $RhoA^{E3.10}/RhoA^{72O}$ trans-heterozygous embryos. (A) The wild-type larva exhibits an internalized head skeleton and intact cuticle at the anterior (arrow) and at the posterior, elongated posterior spiracles (arrowhead). (B–D) Embryos mutant for *RhoA* exhibit similar mutant phenotypes. In all cases a hole on the dorsal side at the anterior of the embryos is apparent (B–D, arrow in B). This hole extends from the anterior to approximately the second or third thoracic segment. (E) Higher magnification of the anterior of the $RhoA^{E3.10}/RhoA^{E3.10}$ homozygous embryo shown in B. The head skeleton has been extruded out of the dorsal opening. In addition to the anterior holes, the shape of the posterior spiracles is aberrant in *RhoA* mutants. (F) Higher magnification of the $RhoA^{E31.0}/RhoA^{E3.10}$ homozygous embryo in B is shown. In contrast to the elongated spiracle in the wild-type larva, *RhoA* mutant embryos exhibit compacted posterior spiracles (B–D, arrowhead in B). The compaction of the posterior spiracle is readily observed in the kinked filzkörper (dark structures within the spiracle). In A–F, anterior is to the left and dorsal is up. The cuticles were imaged by phase contrast microscopy, using a 10× Plan-Neofluar objective (0.3 NA; A–D) or a 20× Achroplan objective (0.45 NA), optivar setting 2× (E and F). Scales are the same in A–D and E and F.

to *RhoA*. Specifically, like the *E3.10* and *J3.8* mutations, *RhoA* excision alleles are recessive embryonic lethals that have defects in the anterior cuticle (Strutt *et al.* 1997).

To test the hypothesis that *E3.10* and *J3.8* are alleles of *RhoA*, we performed complementation analysis between each of the two point mutations, *E3.10* and *J3.8*, and each of two *RhoA* excision alleles, *72F* and *72O* (Strutt *et al.* 1997). Both *E3.10* and *J3.8* fail to complement the *RhoA* excision alleles *72F* and *72O* (Figure 6). Trans-heterozygotes for either of the EMS alleles and either one of the excision alleles are embryonic lethal and give rise to embryos with dorsal anterior holes in the cuticle (Figure 5D). We also mapped the EMS and *RhoA* excision alleles genetically with chromosomal deficiencies. If the previously reported position of *RhoA* (52E3-6) is correct, then $RhoA^{72F}$ and $RhoA^{72O}$ should fail to complement *Df(2R)Jp1*, which uncovers cytogenetic interval 51C3; 52F8-9, but should complement *Df(2R)Jp8*. Flies carrying either *RhoA* excision allele are 100% viable *in trans* to the *Df(2R)Jp1* chromosome, while *Df(2R)Jp8* fails to complement both alleles (Figure 6). This result is consistent with the observed complementation behavior of *E3.10* and *J3.8* with respect to these deficiencies. Finer genetic mapping revealed that *Df(2R)Jp4* (which uncovers cytogenetic interval 51F13; 52F8-9) interacts genetically with zip^{Ebr} at a penetrance of 90% (Table 1). This deficiency also uncovers all four *RhoA* alleles (Figure 6). These results place *RhoA* within cytogenetic interval 52F8-9 (Figure 6). Taken together, these data strongly suggest that mutations *E3.10* and *J3.8* are due to lesions in the *RhoA* locus.

On the basis of these data, we tested the excision *RhoA* alleles for genetic interaction with *zipper*. Both $RhoA^{72F}$ and $RhoA^{72O}$ genetically interact with zip^{Ebr}. Penetrance of the malformed phenotype observed with the *RhoA* mutations ranges from 92 to 96%, comparable to that seen with *Df(2R)Jp4* and slightly lower than that observed with *Df(2R)Jp8*, *E3.10*, and *J3.8* (Table 1). As in the case of the *RhoGEF2-*zip^{Ebr} genetic interactions, 80–90% of the *RhoA-*zip^{Ebr} double heterozygous flies with a malformed leg also exhibit a malformed wing (Figures 3 and 4).

To characterize the nature of the *E3.10* and *J3.8 RhoA* alleles, we examined them for molecular lesions in the *RhoA* locus. We isolated genomic DNA from homozygous *E3.10* and *J3.8* embryos. Genomic fragments were PCR amplified using *RhoA*-specific primers based on the published cDNA sequences (Hariharan *et al.* 1995; Murphy and Montell 1996) and were subsequently sequenced. All intron/exon boundaries spanning the coding region were examined and were found to be wild type. The gene structure differs from that previously published (Figure 7; Strutt *et al.* 1997), but agrees with that reported by Magie *et al.* (1999). In the Strutt study, five exons were identified, excluding one alterna-

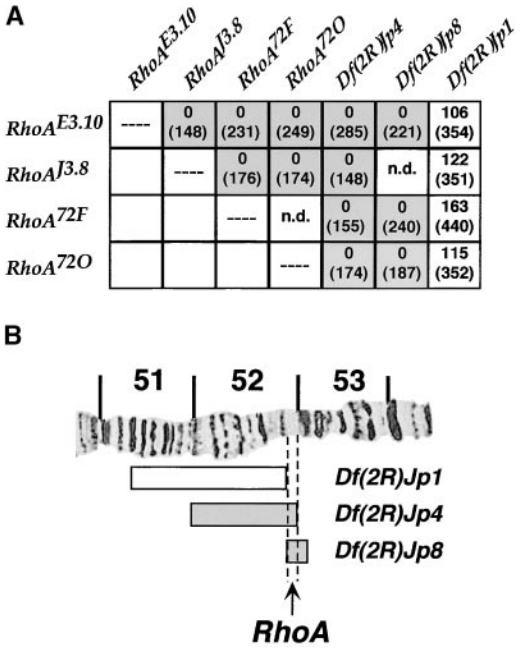

Figure 6.—Finer genetic mapping of the *RhoA* locus. (A) Fail-to-complement tests were performed with the mutations shown. Above the parentheses is the total number of adults recovered that are trans-heterozygous for the indicated mutations (*e.g.*, $RhoA^{E3.10}/RhoA^{J3.8}$). The number in parentheses indicates the total number of progeny recovered in the cross. Because the parental flies are balanced, complementation between mutations is indicated when 33% of adult progeny carry both mutations (see materials and methods). On the basis of this criterion, the *E3.10* and *J3.8* mutations fail to complement known *RhoA* alleles. (B) On the basis of the complementation data in A, the *RhoA* locus fails to complement *Df(2R)Jp4* and *Df(2R)Jp8* and fully complements *Df(2R)Jp1*. This places the RhoA locus at cytogenetic position 52F8-9, on the basis of the cytology defined for these deficiencies (Saxton *et al.* 1991).

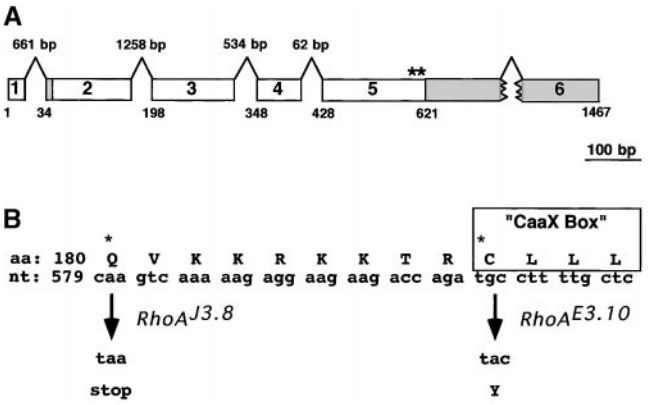

Figure 7.—Genomic organization of the *RhoA* locus and the molecular lesions in $RhoA^{E3.10}$ and $RhoA^{J3.8}$. (A) We sequenced the coding region and exon/intron boundaries of the *RhoA* gene. We identified 5 exons. The sixth exon, encoding the end of the 3′ UTR, was not analyzed. Sizes of the introns were first estimated on the basis of the lengths of PCR products generated from genomic DNA templates or by sequencing through the entire intron. The exact sizes for all of the introns were determined by aligning the exon sequences with genomic sequence generated by the Berkeley Drosophila Genome Project (accession no. AC004248; Berkeley Drosophila Genome Project, unpublished results). In addition, this alignment confirms the exon/intron structure we have determined. The open boxes indicate coding sequences and shaded boxes represent the untranslated sequences. In contrast, Strutt *et al.* (1997) identified only four exons, two of which include protein coding sequence. Asterisks at the end of the coding sequence in exon 5 indicate the site of the molecular lesions in $RhoA^{J3.8}$ and $RhoA^{E3.10}$. (B) Single base changes in the *RhoA* gene are found in the $RhoA^{J3.8}$ (Q180stop) and $RhoA^{E3.10}$ (C189Y) alleles. The last 13 amino acids of RhoA are shown.

tive 5′ exon that we did not examine. We identified six exons of the sizes and organization shown in Figure 7. We definitively defined the exon boundaries by DNA sequencing. These exons include the 5′ UTR, all coding sequences, and the most 5′ portion of the 3′ UTR. However, we did not examine the exon structure of the entire 847-bp 3′ UTR. *E3.10* and *J3.8* each have a single point mutation within the coding sequence in exon 5 (Figure 7). Each mutation is a base substitution of the transition class, consistent with their induction by EMS (Figure 7; Ashburner 1989). *J3.8* is a nonsense mutation at amino acid 180 that results in a protein truncated for the last 13 amino acids. *E3.10* is a missense mutation that encodes a tyrosine residue instead of the cysteine at position 189, which is normally modified by prenylation (Zhang and Casey 1996; Seabra 1998; see discussion). In summary, our genetic and molecular analyses reveal that mutations *E3.10* and *J3.8* are in the *RhoA* gene. We now refer to them as $RhoA^{E3.10}$ and $RhoA^{J3.8}$

***RhoA* mutations interact genetically with *Df(2R)Jp1*:** In the course of mapping the *RhoA* mutations genetically, we observed that *RhoA* mutations interact genetically with *Df(2R)Jp1* (Table 2). This interaction does not require the presence of zip^{Ebr}. All four tested *RhoA* alleles behave as second-site noncomplementors; $RhoA^{E3.10}$ shows the highest penetrance of the malformed phenotype (42%). *Df(2R)Jp1* may delete a portion of the *RhoA* regulatory sequence, leading to interallelic complemen-

TABLE 2

***RhoA* and *Df(2R)Jp1* behave as second-site noncomplementors**

	% malformed (n)[a]	
RhoA allele	*Df(2R)Jp1* +/+ *RhoA*	*Df(2R)Jp1* +/*CyO* and + *RhoA*/*CyO*[b]
$RhoA^{E3.10}$	42 (106)	2 (248)
$RhoA^{J3.8}$	19 (122)	3 (229)
$RhoA^{72F}$	17 (163)	<1 (277)
$RhoA^{72O}$	16 (115)	2 (237)

[a] Percentage of malformed flies double heterozygous for the indicated mutations (*e.g.*, *m* +/+ zip^{Ebr}). *n* is the total number of flies of this genotype that were scored.

[b] Numbers represent the combined total of both genotypic classes.

tation in terms of viability but noncomplementation in terms of mlf, or the *Df(2R)Jp1* chromosome may carry a tightly linked, hypomorphic *RhoA* allele. Alternatively *Df(2R)Jp1* may remove an additional gene or genes required for leg imaginal disc morphogenesis. Interestingly, zip^{Ebr} also interacts genetically with *Df(2R)Jp1* (Halsell and Kiehart 1998). We have also found that *RhoA* mutations exhibit second-site noncomplementation with another locus encoding a gene product in the Rho signal transduction pathway (S. R. Halsell, unpublished observations). Taken together, these results suggest that a gene product encoded by a locus within *Df(2R)Jp1* might function in the Rho signal transduction pathway to regulate nonmuscle myosin function.

DISCUSSION

We have taken a genetic screening approach to identify loci encoding gene products critical for myosin function during morphogenesis (this study; Halsell and Kiehart 1998). We examined flies double heterozygous for *zipper* and another mutation for second-site noncomplementation behavior giving rise to a malformed adult leg.

zip^{Ebr} is the most sensitive *zipper* allele in screens for second-site noncomplementation: In pilot screens, we tested a variety of *zipper* alleles for their sensitivity to second-site noncomplementation (J. Fristrom and S. R. Halsell, unpublished results; Halsell and Kiehart 1998). We found that severe *zipper* alleles (null or near null, hereafter referred to as null) do not exhibit second-site noncomplementation behavior. However, zip^{Ebr} and two other hypomorphic alleles did exhibit second-site noncomplementation behavior (Halsell and Kiehart 1998). At least one of the null alleles, zip^{2}, contains a premature stop codon leading to a truncation of the protein within the head region (Mansfield *et al.* 1996). zip^{2} homozygous mutant embryos have little or no discernable myosin heavy chain protein (Figure 2B; Young *et al.* 1993). To determine the molecular basis of the genetic behavior of zip^{Ebr}, we examined the level of myosin heavy chain protein in homozygous mutant animals by immunoblotting. While the level of protein in mutant embryos is slightly reduced as compared to wild-type animals, homozygous mutant larvae exhibit similar levels when compared to their phenotypically wild-type, heterozygous siblings (Figure 2, D and E). This contrasts with the loss of myosin heavy chain protein found with the genetically noninteracting *zipper* null alleles. This result suggests that a simple reduction in the level of myosin heavy chain in heterozygous flies does not give rise to second-site noncomplementation behavior.

In addition to determining myosin heavy chain protein levels, we also sequenced the zip^{Ebr} allele. We identified a single missense mutation that changes an arginine to histidine at amino acid position 276. Interestingly, this arginine is highly conserved in both conventional and unconventional myosin heavy chains (Cope and Hodge 2000). Mutations in the human myosin VIIA gene that change this arginine residue (human: amino acid 241) to serine give rise to the autosomal recessive congenital deafness and blindness disorder, Usher syndrome type 1B (Janecke *et al.* 1999). In the mouse myosin VII gene, *shaker-1*, this same arginine residue (mouse: amino acid 241) is mutated to proline and this mutation is also associated with deafness (Gibson *et al.* 1995). Based on the solved structure of the chicken skeletal myosin head domain, this arginine (chicken: amino acid 274) lies near the wall of the ATP-binding pocket and may be required to maintain the integrity of this key structure in the native myosin molecule (Rayment *et al.* 1993). As such, this mutated amino acid may affect myosin activity. Myosin heavy chains dimerize in the native myosin molecule. Considering the immunoblot and DNA sequence data, we predict that zip^{Ebr} heterozygous flies carry a mixed population of myosin heavy dimers, including wild-type homodimers, mutant homodimers, and wildtype/mutant heterodimers. We hypothesize that this mixed population of myosin heavy chain dimers gives rise to the genetic sensitivity observed in zip^{Ebr} heterozygous flies.

Our studies reveal that the Rho signal transduction pathway and myosin play essential roles during Drosophila leg and wing morphogenesis: Additional morphogenetic processes are likely to require collaboration between myosin and the Rho signaling pathway. We previously showed that viability depends on myosin and RhoA function; flies double heterozygous for zip^{Ebr} and *RhoA* alleles *E3.10* (C189Y) or *J3.8* (Q180stop) exhibit substantially reduced viability (16 and 50% of Mendelian expectation, respectively; Halsell and Kiehart 1998). We have not yet determined the phenotype of arrest in these animals. Most significantly, our experiments provide direct, genetic evidence supporting the prediction that Rho-mediated regulation of myosin activity is critical for morphogenetic cell shape change.

The mutation in the $RhoA^{E3.10}$ allele disrupts the CaaX box: $RhoA^{E3.10}$ genetically behaves as a severe allele, yet molecularly results from a single amino acid change that converts a cysteine at position 189 to a tyrosine residue. This missense mutation causes severe effects because it alters the first residue, cysteine, in the CaaX box. The CaaX box is a common feature of members of the Ras-superfamily of small GTPases (reviewed in Valencia *et al.* 1991). Functionally, the cysteine residue is the site of a post-translational prenylation modification (reviewed in Zhang and Casey 1996; Seabra 1998). Subsequent to this modification further lipid modifications may occur, and in most cases, the final three amino acids are removed. These modifications are required for proper association of the small GTPase and the membrane; without this association, the GTPase is nonfunctional. These functional relationships have

been demonstrated for numerous Ras superfamily members, including Rho. Site-directed mutagenesis that changes the CaaX box cysteine to serine of the *S. cerevisiae RhoA* homolog, *Rho1*, results in the failure of the mutated *Rho1* protein to repartition from the cytosolic compartment to the membrane (Yamochi *et al.* 1994). Further, these *Rho1* mutant cells fail to grow. In mammalian tissue culture, CaaX box-mutated *RhoB* cannot be lipid modified, and these cells lose their ability to become transformed in sensitized backgrounds (Lebowitz *et al.* 1997). Therefore, it is likely that the $RhoA^{E3.10}$-encoded protein cannot be post-translationally modified, resulting in a complete loss of *RhoA* function. Similarly, the nonsense mutation at residue 180 in the *J3.8* allele would remove the CaaX box and an additional nine amino acids and, therefore, would also behave as a severe *RhoA* allele.

However, on the basis of the differences observed in their genetic interactions with *Df(2R)Jp1* and their levels of reduced viability *in trans* to zip^{Ebr}, $RhoA^{E3.10}$ appears to be a more severe allele than $RhoA^{J3.8}$. We hypothesize that the protein encoded by $RhoA^{E3.10}$ may have a partial dominant-negative effect because it does not repartition properly. On the other hand, the premature stop codon in $RhoA^{J3.8}$. may give rise to an unstable gene product. Since appropriate antibodies directed against Rho are not yet available, we cannot adequately evaluate this alternative.

Myosin, RhoGEF2, and RhoA function in multiple morphogenetic processes: Studies reveal that multiple processes require myosin function throughout Drosophila development, including oogenic cell migrations, larval cytokinesis, and imaginal disc morphogenesis (Gotwals and Fristrom 1991; Karess *et al.* 1991; Edwards and Kiehart 1996; Halsell and Kiehart 1998; this study). Strong or null alleles of *zipper* are embryonic lethal, fail during dorsal closure, and give rise to embryos with dorsal cuticular holes (Young *et al.* 1993). Additionally, myosin immunolocalization studies suggest that myosin is required during stages not yet tested functionally, including embryonic cellularization and gastrulation (Young *et al.* 1991). *RhoGEF2* and *RhoA* also function at least during a subset of the morphogenetic processes that require myosin.

Mutations in the Drosophila *RhoGEF2* gene have been identified by three distinct means: phenotypic suppression of ectopically expressed *RhoA* (Barrett *et al.* 1997), genetic screens for maternally encoded molecules required during early Drosophila embryogenesis (Perrimon *et al.* 1996; Häcker and Perrimon 1998), and genetic screening for molecules required for myosin function (this study). Maternal depletion of *RhoGEF2* results in defects during gastrulation (Barrett *et al.* 1997; Häcker and Perrimon 1998). Specifically, embryos lacking maternal RhoGEF2 fail during apical constriction of ventral furrow cells. Interestingly, myosin localizes to the apical ends of these ventral furrow cells (Young *et al.* 1991; Leptin *et al.* 1992; P. E. Young and D. P. Kiehart, unpublished observations). This observation coupled with the genetic interaction between *RhoGEF2* and myosin during leg morphogenesis suggests that *RhoGEF2* may exert some of its effect during gastrulation via the activity of myosin in these cells.

RhoA mutations are recessive embryonic lethals. Zygotic depletion of *RhoA* results in an anterior dorsal hole in the cuticle (Figure 5; Strutt *et al.* 1997). This defect has been characterized as a dorsal closure phenotype. Dorsal closure is an embryonic morphogenetic event in which the lateral epidermis moves over the dorsal side of the embryo, ultimately fusing along the midline (Young *et al.* 1993; Campos-Ortega and Hartenstein 1997). If dorsal closure fails, then cuticular holes result. Typically, these holes are more posteriorly localized than those observed in *RhoA* mutants. However, certain *zipper* alleles give rise to cuticular holes that extend from the posterior one-third of the embryo to the anterior end (S. R. Halsell, unpublished observations). These extensive cuticular holes are consistent with the head involution defects observed in *zipper* mutants and may reflect combined defects in head morphogenesis and dorsal closure. Therefore *RhoA* loss-of-function mutations may more accurately represent a particular sensitivity in head morphogenesis to perturbation rather than being dorsal closure mutants *per se*.

Nonetheless *RhoA* function during dorsal closure has been implicated by analysis of embryos expressing dominant negative *RhoA* transgenes (Harden *et al.* 1999; Lu and Settleman 1999). In wild-type embryos, the leading-edge cells and the adjacent lateral cells elongate during dorsal closure (Young *et al.* 1993). When dominant-negative *RhoA* is driven in the leading edge by utilizing the GAL-4 UAS system (Brand and Perrimon 1993), stretching of the leading cells initiates but is ultimately lost, and the lateral cells never elongate (Lu and Settleman 1999). The Jun-kinase signal transduction cascade acts during dorsal closure and induces expression of the TGFβ gene, *decapentaplegic* (*dpp*), in the leading-edge cells (reviewed in Noselli 1998). Leading-edge *dpp* expression is a prerequisite for elongation of the flanking lateral cells. In the dominant-negative *RhoA* embryos, *dpp* expression is wild type, therefore the authors suggest that *RhoA* acts upstream of a separate transcriptional pathway (Lu and Settleman 1999). On the basis of our and other data, we suggest that *RhoA* may function directly upstream of myosin in the leading edge. First, we show here that RhoA signaling is necessary for myosin-driven cell shape changes during leg imaginal disc morphogenesis. Second, *zipper* mutants lose myosin in the leading-edge cells, and, subsequently, the leading-edge cells fail to elongate (Young *et al.* 1993). Finally, myosin is delocalized in leading-edge cells expressing dominant negative *RhoA* (Harden *et al.* 1999). Taken together, these results suggest that RhoA signaling may have a direct cellular output at the level

of myosin activity in the leading-edge cells and may not exert its effect via a transcriptional pathway.

Evidence that actomyosin dynamics are regulated by Rho: Numerous pharmacological, cell culture, and biochemical studies implicate the Rho subfamily of GTPases as signal transducers upstream of actin cytoskeleton rearrangements and myosin regulation (reviewed in Van Aelst and D'Souza-Schorey 1997). In Drosophila, injection of mutant forms of Rho or Cdc42 proteins induces gross malformations in the actomyosin cytoskeleton, disrupting a specialized embryonic cytokinesis known as cellularization (Crawford *et al.* 1998). When dominant-negative *Rac1* is expressed at later stages of embryogenesis, the actomyosin cytoskeleton is disrupted in the leading-edge cells during dorsal closure (Harden *et al.* 1995). In Swiss 3T3 cells, the Rho GTPase induces the formation of actin stress fibers (Ridley and Hall 1992). Further, it has been demonstrated that contractility of the actin cytoskeleton, presumably mediated by myosin, is required for stress fiber formation and that this contractility is downstream of Rho signal transduction (Chrzanowska-Wodnicka and Burridge 1996).

In metazoans, nonmuscle myosin and smooth muscle-based contractility depend on the phosphorylation state of the noncovalently bound regulatory light chain (reviewed in Tan *et al.* 1992; Jordan and Karess 1997; J. Crawford, K. A. Edwards and D. P. Kiehart, unpublished results). Molecularly, activated Rho may modulate the phosphorylation state of the regulatory light chain. Biochemical analysis reveals that activated Rho binds and activates a variety of effectors, including a group of serine/threonine kinases known as Rho kinase/ROK and p160ROCK/ROKβ (Leung *et al.* 1995, 1996; Ishizaki *et al.* 1996; Matsui *et al.* 1996). *In vitro* biochemical assays reveal that Rho kinase can phosphorylate the regulatory light chain at its activating sites and induce myosin activity (Amano *et al.* 1996; Kureishi *et al.* 1997). Further, Rho kinases phosphorylate the myosin binding subunit of myosin phosphatase and thus repress its activity; the net result is a further increase in the phosphorylation state of the regulatory light chain (Kimura *et al.* 1996).

Genetic screens in *C. elegans* indirectly implicate regulation of myosin by Rho: Genetic screens for morphogenesis defects in *C. elegans* have identified mutations in loci encoding Rho signal transduction components (Wissmann *et al.* 1997). Mutations in the *C. elegans* Rho kinase locus, *let-502*, disrupt embryonic elongation, while mutations in the regulatory subunit of the myosin phosphatase gene, *mel-11*, suppress the *let-502* morphogenetic defect (Wissmann *et al.* 1997). These results suggest that Rho signal transduction is upstream of myosin-driven morphogenesis in *C. elegans*. This hypothesis cannot be tested directly because myosin mutations that affect cell sheet morphogenesis have not been identified in *C. elegans*. Nonmuscle myosin is encoded by more than one locus and functional redundancy of these loci may preclude the isolation of morphogenetic myosin mutations. In contrast, we were able to screen for mutations that dominantly interact with the *zipper* locus that encodes the myosin heavy chain. Our approach biases our screens toward identifying loci whose gene products may directly affect myosin function. Thus, our studies provide genetic evidence consistent with Rho signal transduction acting directly upstream of myosin activity and bridge the previous *in vitro* and *in vivo* analyses.

Specificity of the *RhoA* and *zipper* interaction: Our genetic analyses reveal that *RhoA* and *RhoGEF2* genetically interact with *zipper*. Comparison of the cytogenetic locations of other loci encoding Rho subfamily components to genomic regions shown to uncover loci that interact genetically with *zipper* (Halsell and Kiehart 1998) indicate that these loci probably do not interact in this screen on the basis of leg morphogenesis. This includes *Rac1* (map position 61F5) and *Rac2* (map position 66A1; Harden *et al.* 1995). Thus, null alleles of *Rac* are unlikely to interact with *zipper*. Drosophila *Cdc42* maps to cytogenetic position 18E1-2, and two strong loss-of-function alleles and one dominant-negative allele of *Cdc42* have been identified (Fehon *et al.* 1997). Neither of the two strong loss-of-function alleles of *Cdc42* exhibit second-site noncomplementation with *zipper* (S. R. Halsell, unpublished results). Interestingly, the dominant-negative allele of *Cdc42* does interact with *zipper* (S. R. Halsell, unpublished results). This result suggests that Cdc42 function may be required for leg morphogenesis or that the dominant-negative form may titrate factors shared with RhoA.

A closely related *RhoA* gene, *Rho-like* (*RhoL*), maps to cytogenetic interval 85D10-12 (Sasamura *et al.* 1997). Previous screens for *zipper* interactions with this genomic region do not reveal an interacting locus (Halsell and Kiehart 1998). Similarly, a Rho-type guanine exchange factor, *rtGEF*, also maps to a genomic region that is noninteracting with *zipper* (Werner and Manseau 1997; Halsell and Kiehart 1998). Finally, a putative Drosophila Rho/Rac effector, *protein kinase N* (*pkn*), has been identified (Lu and Settleman 1999). With low penetrance, *pkn* mutants give rise to embryos with cuticular defects that resemble those of *RhoA* mutants (Lu and Settleman 1999). This locus maps to 45C1, but our previous genomic screens did not test this region (Halsell and Kiehart 1998). However, its binding to the GTP-bound forms of Rac1, Rac2, and RhoA and its slight effect on dorsal closure suggest that *pkn* may function as an effector of Rac or that it may be a redundant effector during dorsal closure. As such, it may not function during leg imaginal disc morphogenesis.

The genetic interaction between the *RhoA* mutant alleles and *Df(2R)Jp1* suggests that additional components of the RhoA signaling pathway may be identified in future screens for the malformed leg phenotype. For example, *Rho kinase* represents a good candidate locus

for interaction. Thus, the specificity of the interactions observed in this study suggests that future screens based on the malformed leg phenotype could identify gene products that function in concert with the RhoA signaling pathway during morphogenetic cell shape changes.

Conclusion: Our genetic screening methods prove highly efficient in identifying mutations that disrupt morphogenesis and in linking them in cellular pathways. These genetic studies greatly extend biochemical and tissue culture analyses, providing direct biological relevance to these assays.

We thank M. Mlodzik, B. Saxton, J. Settleman, and R. Steward for providing mutant stocks. We appreciate the stimulating discussions with the members of the Kiehart lab and critical reading of the manuscript by C. Berg, J. Bloor, B. Capel, J. Crawford, and R. Fehon. This work was supported by National Institutes of Health grants to D.P.K. (GM33830) and S.R.H (GM17383).

LITERATURE CITED

Amano, M., M. Ito, K. Kimura, Y. Fukata, K. Chihara *et al.*, 1996 Phosphorylation and activation of myosin by Rho-associated kinase (Rho-kinase). J. Biol. Chem. **271:** 20246–20249.

Ashburner, M., 1989 *Drosophila: A Laboratory Handbook*. Cold Spring Harbor Laboratory Press, Cold Spring Harbor, NY.

Barrett, K., M. Leptin and J. Settleman, 1997 The Rho GTPase and a putative RhoGEF mediate a signaling pathway for the cell shape changes in Drosophila gastrulation. Cell **91:** 905–915.

Bi, E., P. Maddox, D. J. Lew, E. D. Salmon, J. N. McMillan *et al.*, 1998 Involvement of an actomyosin contractile ring in *Saccharomyces cerevisiae* cytokinesis. J. Cell Biol. **142:** 1301–1312.

Blake, K. J., G. Myette and J. Jack, 1998 The products of *ribbon* and *raw* are necessary for proper cell shape and cellular localization of nonmuscle myosin in Drosophila. Dev. Biol. **203:** 177–188.

Brand, A. H., and N. Perrimon, 1993 Targeted gene expression as a means of altering cell fates and generating dominant phenotypes. Development **118:** 401–415.

Byers, T. J., R. Dubreuil, D. Branton, D. P. Kiehart and L. S. Goldstein, 1987 Drosophila spectrin. II. Conserved features of the alpha-subunit are revealed by analysis of cDNA clones and fusion proteins. J. Cell Biol. **105:** 2103–2110.

Campos-Ortega, J. A., and V. Hartenstein, 1997 *The Embryonic Development of Drosophila melanogaster*. Springer-Verlag, Berlin/Heidelberg, Germany.

Chrzanowska-Wodnicka, M., and K. Burridge, 1996 Rho-stimulated contractility drives the formation of stress fibers and focal adhesions. J. Cell Biol. **133:** 1403–1415.

Condic, M. L., D. K. Fristrom and J. W. Fristrom, 1990 Apical cell shape changes during Drosophila imaginal leg disc elongation: a novel morphogenetic mechanism. Development **111:** 23–33.

Cope, J., and T. Hodge, 2000 The myosin home page. http://www.mrc-lmb.cam.ac.uk/myosin/myosin.html.

Côté, S., A. Preiss, J. Haller, R. Schuh, A. Kienlin *et al.*, 1987 The *gooseberry-zipper* region of Drosophila: five genes encode different spatially restricted transcripts in the embryo. EMBO J. **6:** 2793–2801.

Crawford, J. M., N. Harden, T. Leung, L. Lim and D. P. Kiehart, 1998 Cellularization in *Drosophila melanogaster* is disrupted by the inhibition of Rho activity and the activation of Cdc42 function. Dev. Biol. **204:** 151–164.

De Lozanne, A., and J. A. Spudich, 1987 Disruption of the Dictyostelium myosin heavy chain by homologous recombination. Science **236:** 1086–1091.

Edwards, K. A., and D. P. Kiehart, 1996 Drosophila nonmuscle myosin II has multiple essential roles in imaginal disc and egg chamber morphogenesis. Development **122:** 1499–1511.

Fehon, R. G., T. Oren, D. R. Lajeunesse, T. E. Melby and B. M. McCartney, 1997 Isolation of mutations in the Drosophila homologues of the human Neurofibromatosis 2 and yeast CDC42 genes using a simple and efficient reverse-genetic method. Genetics **146:** 245–252.

Gibson, F., J. Walsh, P. Mburu, A. Varela, K. A. Brown *et al.*, 1995 A type VII myosin encoded by the mouse deafness gene *Shaker-1*. Nature **274:** 62–64.

Gloor, G. B., C. R. Preston, D. M. Johnson-Schlitz, N. A. Nassif, R. W. Phillis *et al.*, 1993 Type I repressors of P element mobility. Genetics **135:** 81–95.

Gotwals, P. J., 1992 Genetic interactions identify genes involved in Drosophila imaginal disc morphogenesis. Ph.D. Thesis, University of California at Berkeley.

Gotwals, P. J., and J. W. Fristrom, 1991 Three neighboring genes interact with the *Broad-complex* and *Stubble-stubbloid* locus to affect imaginal disc morphogenesis in Drosophila. Genetics **127:** 747–759.

Häcker, U., and N. Perrimon, 1998 *DRhoGEF2* encodes a member of the Dbl family of oncogenes and controls cell shape changes during gastrulation in Drosophila. Genes Dev. **12:** 274–284.

Halsell, S. R., and D. P. Kiehart, 1998 Second-site noncomplementation identifies genomic regions required for Drosophila nonmuscle myosin function during morphogenesis. Genetics **148:** 1845–1861.

Harden, N., H. Y. Loh, W. Chia and L. Lim, 1995 A dominant inhibitory version of the small GTP-binding molecule Rac disrupts cytoskeletal structures and inhibits developmental cell shape changes in Drosophila. Development **121:** 903–914.

Harden, N., M. Ricos, Y. M. Ong, W. Chia and L. Lim, 1999 Participation of small GTPases in dorsal closure of the Drosophila embryo: distinct roles for Rho subfamily proteins in epithelial morphogenesis. J. Cell Sci. **112:** 273–284.

Hariharan, I. K., K.-Q. Hu, H. Asha, A. Quintanilla, R. M. Ezzell *et al.*, 1995 Characterization of the rho GTPase family homologues in *Drosophila melanogaster*: overexpressing *Rho1* in retinal cells causes a late developmental defect. EMBO J. **14:** 292–302.

Ishizaki, T., M. Maekawa, K. Fujisawa, K. Okawa, A. Iwamatsu *et al.*, 1996 The small GTP-binding protein Rho binds to and activates a 160 kDa Ser/Thr protein kinase homologous to myotonic dystrophy kinase. EMBO J. **15:** 1885–1893.

Jack, J., and G. Myette, 1997 The genes *raw* and *ribbon* are required for proper shape of tubular epithelial tissues in *Drosophila*. Genetics **147:** 243–253.

Janecke, A. R., M. Meins, M. Sadeghi, K. Grundmann, E. Apfelstedt-Sylla *et al.*, 1999 Twelve novel myosinVIIA mutations in 34 patients with Usher Syndrome Type I: confirmation of genetic heterogenity. Hum. Mutat. **13:** 133–140.

Jordan, P., and R. Karess, 1997 Myosin light chain-activating phosphorylation sites are required for oogenesis in Drosophila. J. Cell Biol. **139:** 1805–1819.

Karess, R. E., X. Chang, K. A. Edwards, S. Kulkarni, I. Aguilera *et al.*, 1991 The regulatory light chain of nonmuscle myosin is encoded by *spaghetti-squash*, a gene required for cytokinesis in Drosophila. Cell **65:** 1177–1189.

Ketchum, A. S., C. T. Stewart, M. Stewart and D. P. Kiehart, 1990 Complete sequence of the Drosophila nonmuscle myosin heavy-chain transcript: conserved sequences in the myosin tail and differential splicing in the 5′ untranslated sequence. Proc. Natl. Acad. Sci. USA **87:** 6316–6320.

Kiehart, D. P., and R. Feghali, 1986 Cytoplasmic myosin from *Drosophila melanogaster*. J. Cell Biol. **103:** 1517–1525.

Kiehart, D. P., R. A. Montague, W. L. Rickoll, D. Foard and G. H. Thomas, 1994 High-resolution microscopic methods for the analysis of cellular movements in Drosophila embryos, pp. 507–532 in *Drosophila melanogaster: Practical Uses in Cell and Molecular Biology*, edited by L. S. B. Goldstein and E. A. Fyrberg. Academic Press, San Diego.

Kiehart, D. P., C. G. Galbraith, K. A. Edwards, M. P. Sheetz, W. Rickoll *et al.*, 2000 Multiple forces contribute to cell sheet morphogenesis for dorsal closure in Drosophila. J. Cell Biol. **149:** 471–490.

Kimura, K., M. Ito, M. Amano, K. Chihara, Y. Fukata *et al.*, 1996 Regulation of myosin phosphatase by Rho and Rho-associated kinase (Rho-kinase). Science **273:** 245–248.

Knecht, D. A., and W. F. Loomis, 1987 Antisense RNA inactivation of myosin heavy chain in *Dictyostelium discoideum*. Science **236:** 1081–1086.

Knecht, D. A., and E. Shelden, 1995 Three-dimensional localiza-

tion of wild-type and myosin II mutant cells during morphogenesis of Dictyostelium. Dev. Biol. **170:** 434–444.

Kureishi, Y., S. Kobayashi, M. Amano, K. Kimura, H. Kanaide *et al.*, 1997 Rho-associated kinase directly induces smooth muscle contraction through myosin light chain phosphorylation. J. Biol. Chem. **272:** 12257–12260.

Lebowitz, P. F., W. Du and G. C. Prendergast, 1997 Prenylation of RhoB is required for its cell transforming function but not its ability to activate serum response element-dependent transcription. J. Biol. Chem. **272:** 16093–16095.

Leptin, M., J. Casal, B. Grunewald and R. Reuter, 1992 Mechanisms of early Drosophila mesoderm formation. Development (Suppl.), 23–31.

Leung, T., E. Manser, L. Tan and L. Lim, 1995 A novel serine/threonine kinase binding the ras-related RhoA GTPase which translocates the kinase to peripheral membranes. J. Biol. Chem. **256:** 29051–29054.

Leung, T., X.-Q. Chen, E. Manser and L. Lim, 1996 The p160 RhoA-binding kinase ROKa is a member of a kinase family and is involved in the reorganization of the cytoskeleton. Mol. Cell. Biol. **16:** 5313–5327.

Lis, J. T., J. A. Simon and C. A. Sutton, 1983 New heat shock puffs and beta-galactosidase activity resulting from transformation of Drosophila with an hsp70-lacZ hybrid gene. Cell **35:** 403–410.

Lu, Y., and J. Settleman, 1999 The Drosophila Pkn protein kinase is a Rho/Rac effector target required for dorsal closure during embryogenesis. Genes Dev. **13:** 1168–1180.

Magie, C. R., M. R. Meyer, M. S. Gorsuch and S. M. Parkhurst, 1999 Mutations in the *Rho1* small GTPase disrupt morphogenesis and segmentation during early Drosophila development. Development **126:** 5353–5364.

Mansfield, S. G., D. Y. Al-Shirawi, A. S. Ketchum, E. C. Newbern and D. P. Kiehart, 1996 Molecular organization and alternative splicing in *zipper*, the gene that encodes the Drosophila nonmuscle myosin II heavy chain. J. Mol. Biol. **255:** 98–109.

Manstein, D., M. Titus, A. Delozanne and J. Spudich, 1989 Gene replacement in Dictyostelium—generation of myosin null mutants. EMBO J. **8:** 923–932.

Matsui, T., M. Amano, T. Yamamoto, K. Chihara, M. Nakafuku *et al.*, 1996 Rho-associated kinase, a novel serine/threonine kinase, as a putative target for the small GTP binding protein Rho. EMBO J. **15:** 2208–2216.

Miller, K. G., 1995 Role of the actin cytoskeleton in early Drosophila development, pp. 167–196 in *Current Topics in Developmental Biology*, edited by D. G. Capco. Academic Press, San Diego.

Murphy, A. M., and D. J. Montell, 1996 Cell type-specific roles for Cdc42, Rac, and RhoL in Drosophila oogenesis. J. Cell Biol. **133:** 617–630.

Neujahr, R., C. Heizer and G. Gerisch, 1997 Myosin II-independent processes in mitotic cells of *Dictyostelium discoideum*: redistribution of the nuclei, rearrangement of the actin system and formation of the cleavage furrow. J. Cell Sci. **110:** 123–137.

Noselli, S., 1998 JNK signaling and morphogenesis in Drosophila. Trends Genet. **14:** 33–38.

Pederson, J. D., 1997 Genetic and cellular regulation of embryonic morphogenesis in *Drosophila melanogaster*. Ph.D. Thesis, North Carolina State University.

Pederson, J. D., D. P. Kiehart and J. W. Mahaffey, 1996 The role of HOM-C genes in segmental transformations: reexamination of the Drosophila *sex combs reduced* embryonic phenotype. Dev. Biol. **180:** 131–142.

Perrimon, N., A. Lanjuin, C. Arnold and E. Noll, 1996 Zygotic lethal mutations with maternal effect phenotypes in *Drosophila melanogaster*. II. Loci on the second and third chromosome identified by *P*-element-induced mutations. Genetics **144:** 1681–1692.

Preiss, J. R., and D. I. Hirsh, 1986 *Caenorhabditis elegans* morphogenesis: the role of the cytoskeleton in elongation of the embryo. Dev. Biol. **117:** 156–173.

Rayment, I., W. R. Rypniewski, K. Schmidt-Base, R. Smith, D. R. Tomchick *et al.*, 1993 Three-dimensional structure of myosin subfragment-1: a molecular motor. Science **261:** 50–58.

Ridley, A. J., and A. Hall, 1992 The small GTP-binding protein rho regulates the assembly of focal adhesions and actin stress fibers in response to growth factors. Cell **70:** 389–399.

Sasamura, T., T. Kobayashi, S. Kojima, H. Qadota, Y. Ohya *et al.*, 1997 Molecular cloning and characterization of Drosophila genes encoding small GTPases of the rab and rho families. Mol. Gen. Genet. **254:** 486–494.

Saxton, W. M., J. Hicks, L. S. B. Goldstein and E. C. Raff, 1991 Kinesin heavy chain is essential for viability and neuromuscular functions in Drosophila, but mutants show no defects in mitosis. Cell **64:** 1093–1102.

Schoenwolf, G. C., and J. L. Smith, 1990 Mechanisms of neurulation: traditional viewpoint and recent advances. Development **109:** 243–270.

Seabra, M. C., 1998 Membrane association and targeting of prenylated Ras-like GTPases. Cell. Signaling **10:** 167–172.

Shelden, E., and D. A. Knecht, 1996 Dictyostelium cell shape generation requires myosin II. Cell Motil. Cytoskel. **35:** 59–67.

Strutt, D. I., U. Weber and M. Mlodzik, 1997 The role of RhoA in tissue polarity and Frizzled signalling. Nature **387:** 292–295.

Tan, J. L., S. Ravid and J. A. Spudich, 1992 Control of nonmuscle myosins by phosphorylation. Annu. Rev. Biochem. **61:** 721–759.

Valencia, A., P. Chardin, A. Wittinghofer and C. Sander, 1991 The *ras* protein family: evolutionary tree and role of conserved amino acids. Biochemistry **30:** 4637–4647.

Van Aelst, L., and C. D'Souza-Schorey, 1997 Rho GTPases and signaling networks. Genes Dev. **11:** 2295–2322.

von Kalm, L., D. K. Fristrom and J. Fristrom, 1995 The making of a fly leg: a model for epithelial morphogenesis. BioEssays **17:** 693–702.

Watts, F. Z., B. Sheils and E. Orr, 1987 The yeast MYO1 gene encoding a myosin-like protein required for cell division. EMBO J. **6:** 3499–3505.

Werner, L. A., and L. J. Manseau, 1997 A Drosophila gene with predicted rhoGEF, pleckstrin homology and SH3 domains is highly expressed in morphogenic tissues. Gene **187:** 107–114.

Wheatley, S., S. Kulkarni and R. Karess, 1995 Drosophila nonmuscle myosin II is required for rapid cytoplasmic transport during oogenesis and for axial nuclear migration in early embryos. Development **121:** 1937–1946.

Wieschaus, E., and C. Nüsslein-Volhard, 1986 Looking at embryos, pp. 199–227 in *Drosophila: A Practical Approach*, edited by D. B. Roberts. IRL Press, Oxford.

Williams-Masson, E. M., A. N. Malik and J. Hardin, 1997 An actin-mediated two-step mechanism is required for ventral enclosure of the *C. elegans* hypodermis. Development **124:** 2889–2901.

Wissmann, A., J. Ingles, J. D. McGhee and P. E. Mains, 1997 *Caenorhabditis elegans* LET-502 is related to Rho-binding kinases and human myotonic dystrophy kinase and interacts genetically with a homolog of the regulatory subunit of smooth muscle myosin phosphatase to affect cell shape. Genes Dev. **11:** 409–422.

Yamochi, W., K. Tanaka, H. Nonaka, A. Maeda, T. Musha *et al.*, 1994 Growth site localization of Rho1 small GTP-binding protein and its involvement in bud formation in *Saccharomyces cerevisiae*. J. Cell Biol. **125:** 1077–1093.

Young, P. E., T. C. Pesacreta and D. P. Kiehart, 1991 Dynamic changes in the distribution of cytoplasmic myosin during Drosophila embryogenesis. Development **111:** 1–14.

Young, P. E., A. M. Richman, A. S. Ketchum and D. P. Kiehart, 1993 Morphogenesis in Drosophila requires nonmuscle myosin heavy chain function. Genes Dev. **7:** 29–41.

Zang, J.-H., G. Cavet, J. H. Sabry, P. Wagner, S. L. Moores *et al.*, 1997 On the role of myosin-II in cytokinesis: division of Dictyostelium cells under adhesive and nonadhesive conditions. Mol. Biol. Cell **8:** 2617–2629.

Zhang, F. L., and P. J. Casey, 1996 Protein prenylation: molecular mechanisms and functional consequences. Annu. Rev. Biochem. **65:** 241–269.

Zhao, D. B., S. Côté, F. Jahnig, J. Haller and H. Jäckle, 1988 *zipper* encodes a putative integral membrane protein required for normal axon patterning during Drosophila neurogenesis. EMBO J. **7:** 1115–1119.

Communicating editor: R. S. Hawley